Estuaries and Coasts (2026) 49:58
https://doi.org/10.1007/s12237-026-01672-y

Compound Minor Flooding and Relative Sea Level Rise in the Lower Winyah Bay Watershed, South Carolina, USA

Madison S. Fink[1] · H.E. Baranes[2] · S. L. Dykstra[3] · S. A. Talke[4] · T. J.J. Hanebuth[1]

Received: 9 May 2025 / Revised: 2 January 2026 / Accepted: 21 January 2026 / Published online: 25 February 2026

Abstract

High-tide flooding is becoming an increasingly common phenomenon in coastal communities. This study characterizes the driving mechanisms and temporal variability of minor flood events in the Lower Winyah Bay Watershed, South Carolina, USA caused by a combination of river discharge, tides, non-tidal residuals (NTR), and relative sea-level rise (RSLR), using a physics-based regression model of daily high-water (DHW). Results showed that all three mechanisms contributed to 534 floods between 2017 and 2024 in Georgetown (23 river km; rkm), either as single-driver floods (2–10% of flood days; range based on associated model error) or compound floods (90–98% of total flood days). Tides dominated 237–244 (45%) floods, river discharge drove 162–186 (33%) floods, and NTR was the primary mechanism contributing to 111–128 (22%) floods. Further upstream at Conway (91 rkm), for the 128 identified flood days, ~87% were single-driver river discharge flood days and only 4–11% were compound flood days. The model further shows frequent flooding within the estuary is driven by high RSLR rates of 11.3 ± 1.7 mm/yr at Georgetown and 14.4 ± 1.9 mm/yr at Conway. By comparison, the rate of DHW rise at the coast is 8.6 ± 4.3 mm/yr. We project that by 2041, the flood frequency will increase by 249% in Georgetown and ~160% in Conway. Our results demonstrate the increasingly chronic nature of flooding and the need for low-lying communities along tidal rivers to account for both marine and fluvial processes, including RSLR, in future adaptation planning.

Keywords Compound flooding · Nuisance flooding · Tidal river · River flow · Flood threshold · Relative sea level rise

Introduction

Low-lying coastal and estuarine regions are subject to flood risk due to the combination of tides, river discharge, coastal ocean dynamics, and a rising sea level (McKeon & Piecuch, 2025). Coastal drivers of flooding, including relative sea level rise (RSLR), tides, and storm surge, can also propagate more than 100–200 km inland along estuaries and tidal rivers (e.g., Ralston et al., 2019; Baranes et al., 2023; Dykstra et al., 2022). However, characterizing flood risk for local communities in the inland portions of these systems is challenging due to the interactions among marine, hydrologic, and atmospheric forcing mechanisms, as well as the local hydrodynamic response, which can shift over time due to dredging, wetland reclamation and other local interventions (e.g., Talke et al., 2021).Global-scale compound coastal-riverine flood modeling studies have found that the impacts of compound flooding are likely to increase due to climate-induced sea-level rise (Wahl et al., 2015; Bevacqua et al., 2019). This increasing frequency and duration of minor flooding impacts ecosystems, infrastructure, and human lives (Hino et al., 2019).

Minor flooding is becoming an increasingly common phenomenon in coastal communities (e.g., Sweet et al., 2018). *Minor flooding* can be driven by many processes and is not driver-specific (e.g., "high-tide", "nuisance", or

Communicated by Arnoldo Valle-Levinson

✉ Madison S. Fink
msfink@coastal.edu

[1] Department of Marine Science, Coastal Carolina University, Conway, SC 29528, USA

[2] Gulf of Maine Research Institute, Climate Center, Portland, ME 04101, USA

[3] College of Fisheries and Ocean Science, University of Alaska Fairbanks, Fairbanks, AK 99775, USA

[4] Department of Civil and Environmental Engineering, California Polytechnic State University, San Luis Obispo, CA 93407, USA

"sunny-day" flooding). A variety of empirically derived and impact-based thresholds have been used to quantify flooding and its frequency along the coast globally. The National Weather Service (NWS) has used local reports of impacts, such as roads flooding and beach erosion, to identify minor, moderate, and major flood thresholds for locations in the United States. The National Ocean Service (NOS) has used the relationship between tidal range and tidal datums to empirically derive flood thresholds for coastal gauges (Moftakhari et al., 2015, 2024; Sweet et al., 2018; Piecuch et al., 2025). Further work has improved the study of minor flooding, including developing statistical models for impact-based thresholds that account for uncertainty, and using innovative techniques, like social media, to capture local flood impacts (Moore & Obradovich, 2020; Piecuch et al., 2025). Along the East Coast of the United States, high tide flood frequency increased by 75 to 125% since 2000 (Sweet et al., 2018). While this increase is caused primarily by RSLR, changes to tidal properties also impact the number of flood events, particularly in estuaries (e.g., Li et al., 2021; De Leo et al., 2022; Pareja-Roman et al., 2023).

The global rate of sea-level rise has increased over the last several decades to 3.3 mm/year from 1993 to 2023, and is accelerating at about 0.08 mm/yr^2 (Nerem et al., 2018; Hamlington et al., 2024). Projections of future nuisance flooding scenarios based on estimates of future RSLR suggest that these trends will accelerate, with chronic flooding (>50 floods per year) common in many locations by mid-century (Sweet & Park, 2014; Sweet et al., 2018; Morris & Renken, 2020; Thompson et al., 2021). In some regions, climate change may also be increasing the annual frequency of extreme precipitation events and thus discharge events, including the Southeastern United States (Armal et al., 2018; Dykstra & Dzwonkowski, 2021). In 2018, Hurricane Florence slowly moved over South Carolina, North Carolina, and Virginia, causing coastal and riverine flooding that flooded properties valued at $52 billion (Tedesco et al., 2020). In these states, most new construction is concentrated in coastal counties where flood exposure continues to increase.

While there is a growing body of literature on the mechanisms leading to compound flood events, these studies primarily use measurements at or near open seas and do not adequately represent the more inland regions where compound flood drivers are more likely to interact (Dykstra & Dzwonkowski, 2021). Due to the changing nature of the fluvial and marine drivers of coastal and estuarine flooding, it is important to characterize their impact on flood risk. Many studies have investigated the role of inland fluvial forcing mechanisms in compound flood events (Serafin et al., 2019; Moftakhari et al., 2019; Baranes et al., 2023). Locally, the spatial pattern of tidal and storm surge amplitude is influenced by regional river characteristics, including topography and system geometry. Long-term changes in these factors alter how estuarine and tidal river water levels respond to tides and discharge (e.g., Dykstra & Dzwonkowski, 2021; Helaire et al., 2019; Talke et al., 2021). Examining the relative contributions of physical drivers, such as discharge, tides, and wind, at a smaller spatial scale allows these local details to be considered when analyzing flood hazards. Hydrodynamic, statistical, and numerical modeling have been conducted at the watershed scale to characterize compound flood hazards in estuarine systems, including examples such as the Yangtze River, San Francisco Bay, and Delaware Bay (Guo et al., 2015; Tehranirad et al., 2020; Xiao et al., 2021). Nederhoff et al. (2021) used a numerical hydrodynamic model, and found that tides and non-tidal residual variations had the most significant impact on extreme water levels in the South and Central San Francisco Bay, while fluvial inputs played an increasingly important role in the North Bay and Sacramento-San Joaquin Delta. In estuaries and tidal rivers, Moftakhari et al. (2019) applied a joint statistical and hydrodynamic approach and found that nonlinear interactions between discharge and tides are important in generating flooding upstream. Physical models for flood inundation mapping are being improved with machine learning through the use of neural networks to increase resolution (Jafarzadegan et al., 2023). Although using more complex statistical, numerical, or machine learning methods could increase the accuracy and efficiency of flood forecasting, we opt for a simpler, physically interpretable model. This approach allows us to describe the geographical variability in compound flooding rather than focusing on the accurate forecast or hindcast of specific events.

Characterizing the more frequent minor compound flood events is a critical step necessary in flood hazard assessment, which is accomplished here by focusing on the Northern region of South Carolina using historical data and a statistical framework. Our study applies a physics-based regression approach to differentiate the relative contributions of RSLR, non-tidal coastal water level variability (i.e., non-tidal residual, NTR), river discharge, and tides to minor flooding along the tidal rivers of the Winyah Bay watershed, an estuary. The regression analysis also allows for the isolation of a locally accurate RSLR rate (which may differ from the coastal rate) from other forcing mechanisms (Baranes et al., 2023). The regression-derived RSLR rates and river discharge contributions to minor floods are used to assess how future sea level rise, vertical land motion, and changes in river discharge may impact flood hazard for communities along the estuaries and tidal rivers.

Setting

In the Southeastern US, RSLR rates can significantly exceed the global average due to land subsidence and regional ocean dynamics. Dangendorf et al. (2023) found that sterodynamic effects have driven rates of RSLR exceeding 10 mm/yr in the Southeast since 2010. In coastal South Carolina, relative subsidence rates up to 6 mm/yr (Ohenhen et al., 2024a) further increase RSLR rates. While the variability of vertical land motion in this region has not been well studied, GNSS stations and InSAR data reflect regional variability that could be related to soft sediment compaction, movement of the Cape Fear Arch, or groundwater extraction (Van De Plassche et al., 2014; Karegar et al., 2016; Blewitt et al., 2018; Ohenhen et al., 2024). Climate change is projected to exacerbate river discharge contributions to flooding, with studies on the Pee Dee River Basin indicating a potential 13–43% increase in average daily discharge throughout the year by 2050–2070 (Suttles et al., 2018). Tidal flooding events have also become more prominent in coastal and estuarine areas. Minor flood days at Springmaid Pier in Myrtle Beach, South Carolina have increased from 2 days/year in 2000 to 11 days/year in 2020 and are projected to reach 30–75 days/year by 2050 (Sweet et al., 2021). Consequently, historic communities along the tidal rivers, some of which have persisted for centuries, are experiencing more frequent and impactful flood events.

The Winyah Bay estuary is fed by five coastal rivers: the Pee Dee River, Black River, Lynches River, Waccamaw River and Sampit River (Fig. 1). There is a mean annual

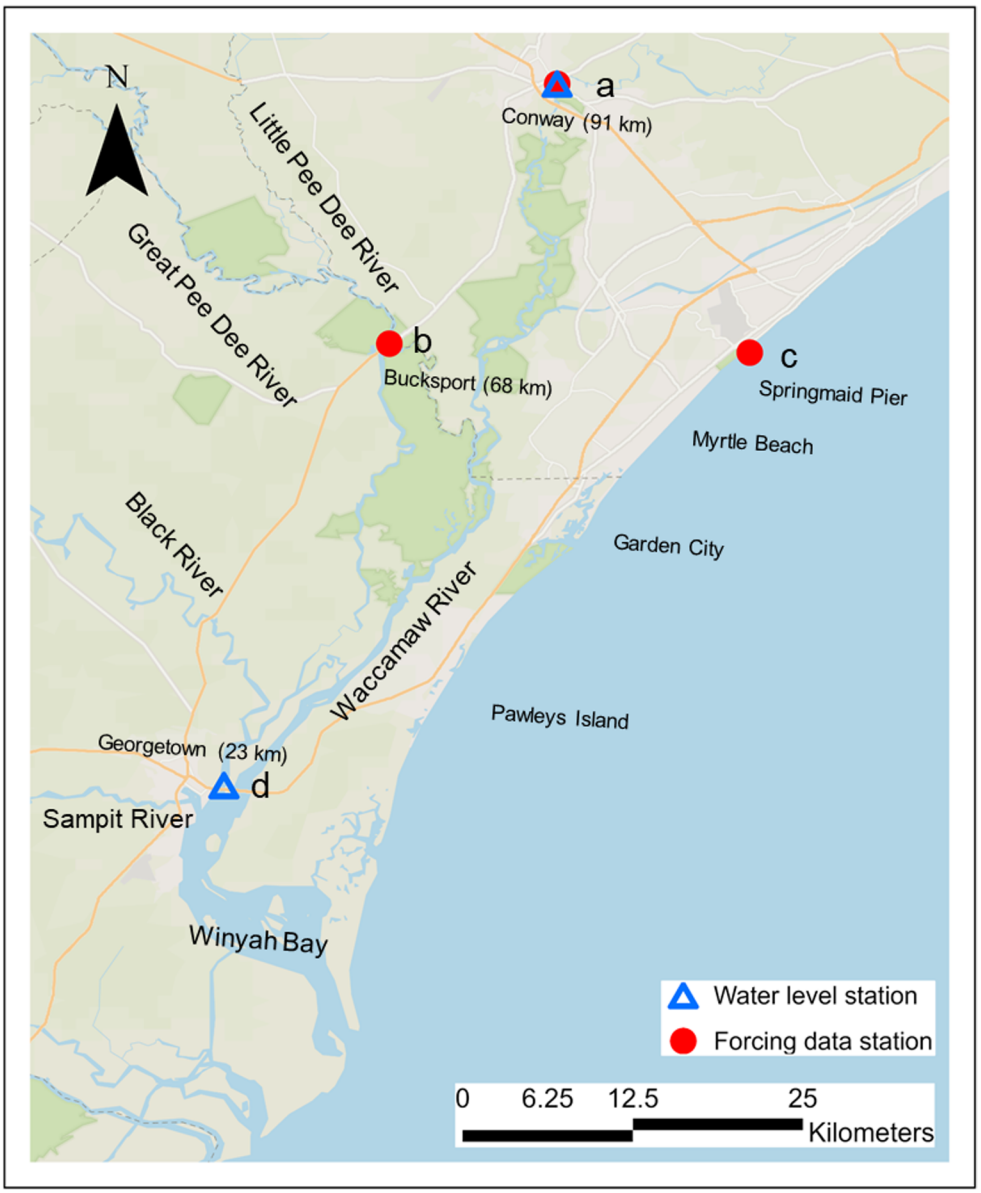

Fig. 1 Map of the Lower Winyah study area highlighting measurement stations used in this study: (**a**) Conway USGS Station (water level; discharge), (**b**) Bucksport USGS station (discharge), (**c**) Springmaid Pier NOAA station (tides, coastal ocean level), (**d**) Georgetown USGS station (water level). The distances reported represent the distance from the station to the estuary mouth. See Table 1 for more information

combined discharge of 510 m^3/s (Dykstra et al., 2024a; Kim & Voulgaris, 2005; Allen et al., 2014). The funnel-shaped bay has a surface area of 155 km^2 and is approximately 30 km long and up to 7.5 km wide. The predominantly semidiurnal tides have a range that decreases from 1.4 m near the mouth to 1.0 m at the confluence of the Waccamaw and Pee Dee Rivers (Patchineelam et al., 1999). All distances inland reference the mouth as river kilometer 0 (i.e., rkm 0). The Winyah Bay watershed area is approximately 47,000 km^2. The Pee Dee River and its two major tributaries, the Black River and Lynches River, account for 86% of the discharge of the Winyah Bay watershed (Fig. 2a). The Pee Dee River watershed originates in the elevated Piedmont region of North Carolina. It flows 400 km across the coastal plains of central North Carolina and northern South Carolina, draining an area of 36,520 km^2 with an average annual river discharge of 390 m^3/s (Dykstra et al., 2024a; Patchineelam et al., 1999). The next largest river system, the Waccamaw River, originates in North Carolina and drains an area of 1,981 km^2 within the Coastal Plain (Ensign et al., 2014). Emergent and forested wetlands are prevalent along the brackish and freshwater portions of the rivers (Allen et al., 2014; Ensign et al., 2014). During low discharge periods, tides can extend up the Waccamaw River more than 118 km inland (United States Geological Survey, USGS 02110550), beyond Conway (rkm 92). In the Pee Dee River, tides can extend above Bucksport (68 km from the mouth of the estuary). Salt can extend up to 42 and 48 km inland in the Pee Dee River and Waccamaw River, respectively, and at high river discharge is restricted to near the estuary mouth (Dykstra et al., 2024a; Elsinger & Moore, 1984; Ensign et al., 2014).

The region surrounding Winyah Bay faces significant flood exposure, partly due to its low-elevation topography. Escalating flood-related issues have substantial economic implications for nearby Myrtle Beach, a major tourist destination attracting over 17 million visitors annually (Visit Myrtle Beach, 2022). The climate-driven increase in sea level and river discharge are also increasing flood hazards, illustrated by recent high-water records in the Black, Pee Dee, and Waccamaw Rivers during hurricanes Matthew and Florence (Griffin et al., 2019). Between 2015 and 2018, major storms like Hurricanes Matthew and Florence caused the Waccamaw and Pee Dee Rivers to exceed their record water levels three separate times. (Griffin et al., 2019). Despite this evident and growing flood risk, understanding the precise mechanisms driving flooding in such tidal rivers and surrounding communities remains challenging due to the complex nature of coastal ocean variability, tides, river discharge, and rising sea level.

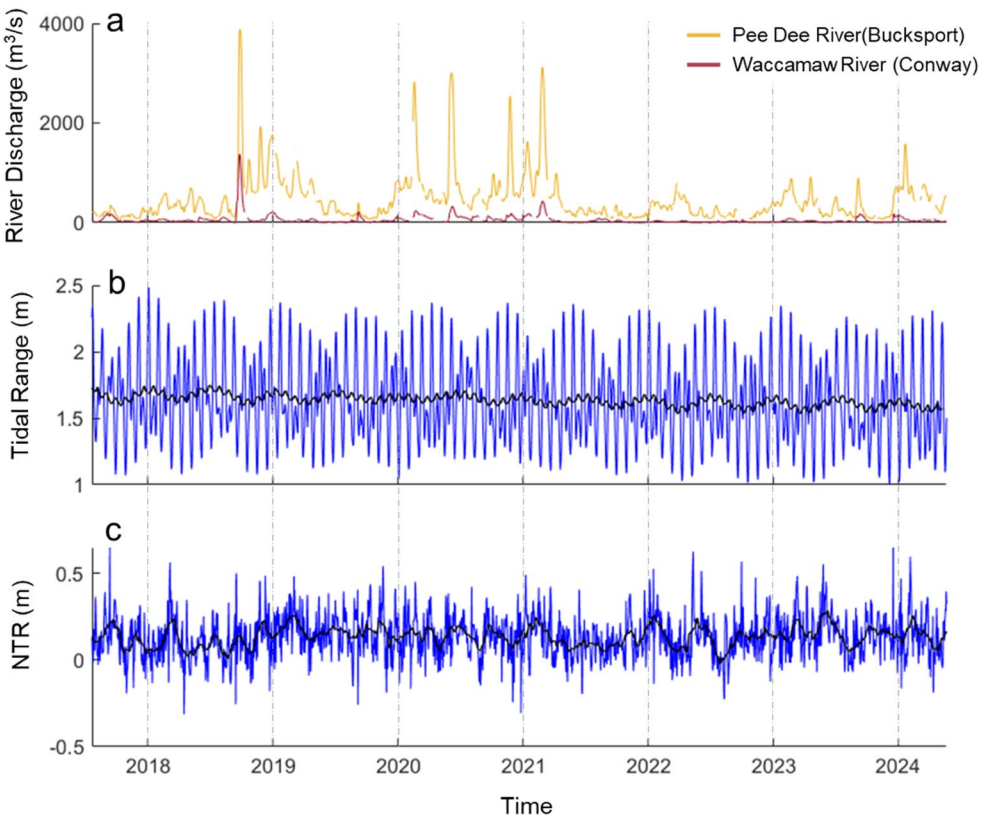

Fig. 2 Model forcing data for the period of analysis (2017–2024). (**a**) Daily-averaged discharge for the Pee Dee River (yellow) and Waccamaw River (red). (**b**) Daily-averaged tidal range from Springmaid Pier. (blue) and monthly-averaged tidal range (black). (**c**) daily-averaged NTR (blue) and monthly-averaged coastal water level (black). See Table 1 for forcing data station locations and sources

Methods

Data

We evaluate the influence of tides, river flow and NTR at two USGS water level gauges: Georgetown (rkm 23) and Conway (rkm 91) (Fig. 1; Table 1). River discharge data is obtained for the Waccamaw River at Conway and for the Pee Dee River at Bucksport (Table 1). River discharge is tidally filtered using a spectral band-pass filter following the USGS protocol (Ruhl & Simpson, 2005). Daily averages are calculated from hourly data for use in the model. Water level measurements from July 21, 2017 to May 21, 2024, are evaluated relative to the North American Vertical Datum of 1988 (NAVD88), with the start date determined by the gauge with the shortest record (Georgetown). While relatively short in duration, this period covers a range of flow, wind, and coastal water level conditions, which lends itself to robust analysis (Fig. 2).

Hourly predicted tidal water level and NTR are calculated using verified hourly water level measurements from the National Oceanic and Atmospheric Administration (NOAA) Springmaid Pier station in Myrtle Beach (Table 1). This coastal station was selected because its measurements are not influenced by river discharge and the lag between the stations does not have an impact at the daily timescale of our model. The measured water level time series is detrended using the linear trend from 2017 to 2024. Tidal predictions are then calculated using the Unified Tidal Analysis and Prediction software (UTide; Codiga, 2011) for each year of data using the standard 68 constituents and nodal/satellite corrections. Each annual analysis is used to reconstruct hourly water levels. The seasonal cycle in water level along the South Atlantic Bight is strongly influenced by the Gulf Stream and is represented well by the SA and SSA constituents with small variability from year-to-year (Parker, 2007). The daily Great Diurnal Tidal Range (GT) is determined as the difference between the daily maximum and minimum predicted water levels (Fig. 2b). The non-tidal residual (NTR), which represents short-time scale coastal sea level variations driven by processes such as wind, pressure, and steric effects, is calculated as the difference between the verified and predicted water levels at the Springmaid Pier station (Fig. 2c). Daily averaged values are subsequently used in the model.

Regression Model

Water levels can be related to their forcing mechanisms using physics-based regression models (Jay & Flinchem, 1997; Kukulka & Jay, 2003; Jay et al., 2011, 2016). These models are based on the theory of tidal propagation in convergent channels with friction and the influence of river discharge. Because these formulations are related to the physical equations that govern how tides and discharge interact, particularly over ranges of discharge and tidal conditions, the models have been applied in a variety of settings. Other studies have used similar statistical formulations, further demonstrating the applicability of these approaches in various system configurations (Matte et al., 2013; Guo et al., 2015). Initial versions considered only tidal and fluvial interactions and their role in influencing daily and monthly mean water levels (Jay & Flinchem, 1997; Kukulka & Jay, 2003). Jay et al. (2016) expanded the model to include the influence of coastal water levels, multiple river flows, and hydropower operations on lower-low water (LLW) and higher-high water (HHW), in addition to mean water level (MWL). Baranes et al. (2023) added additional terms to the model, including wind, RSLR, and freshwater withdrawals. By applying the regression to 50 + tide gauges, Baranes et al. (2023) was able to assess spatial variability in the response of daily MWL to various forcing factors (e.g., coastal variability and river flow) and isolate the RSLR trend from

Table 1 Water level and forcing data source information. See Fig. 1 for the location of stations

Station	Data purpose	Hydrologic system	Distance to mouth of estuary (km)	Data source	Length of record
Conway	water level, discharge	Waccamaw	91	USGS (Station ID 02110704)	2014-present (water level) 2007-present (discharge)
Bucksport	discharge	Pee Dee	68	USGS (Station ID 02135200)	2007-present
Springmaid Pier	NTR, tides, RSLR	Ocean	--	NOAA (Station ID 8661070)	1957-present
Georgetown	water level	Pee Dee	23	USGS (Station ID 02136350)	2017-present

variations in other water level drivers. Templeton et al. (2024) used a similar approach to assess how shallow water habitat in the Lower Columbia River evolved over the last century due to changing river flow, tides, sea-level changes, and subsidence. Unlike a numerical model, a physics-based regression model is computationally simple and does not require bathymetry data. This enables implementation in our study area and an evaluation of the effect of changing conditions on flood event frequency.

Daily high-water (DHW) represents the maximum daily water level, which is a good indicator of when minor flooding might occur. The relationship between DHW and physical forcing mechanisms such as astronomical tides, river flow, and the NTR is determined using a dynamically-based regression model developed by Kukulka and Jay (2003), Jay et al. (2011) and Jay et al. (2016). The model is modified following Baranes et al. (2023) to account for RSLR. DHW, in meters, is calculated as:

$$DHW = \underbrace{a_0}_{1} + \underbrace{a_1 Q_{Waccamaw}^{n1w}}_{2} + \underbrace{a_2 Q_{Pee\ Dee}^{n1p}}_{3} + \underbrace{a_3 T^{n^2} Q_{pw}^{-n3}}_{4} + \underbrace{a_4 C}_{5} + \underbrace{a_5 t}_{6} \quad (1)$$

Equation 1 is evaluated separately for DHW at the Conway and Georgetown stations. Term 1 is the offset of DHW to the NAVD88 vertical datum and is the water level that would occur with no other forcing (i.e., if terms 2–5 had values of zero). Terms 2 and 3 are used to model the influence of river discharge in the two main fluvial systems on water levels. Q is the tidally filtered daily mean river discharge for the Waccamaw and Pee Dee rivers in m^3/s. Term 4 represents the interacting influence on DHW of coastal tidal range T (in meters) and combined Waccamaw-Pee Dee River flow ($Q_{pw} = Q_{Waccamaw} + Q_{Pee\ Dee}$). T is the daily Great Diurnal Range (meters) at Springmaid Pier, and reflects spring-neap, monthly, and seasonal variations in daily peak water level. The total discharge Q_{pw} attenuates a landward propagating tide and decreases term 4 (see e.g., Godin, 1999; Kukulka & Jay, 2003). Term 5 is the NTR variability using the daily mean NTR, C in meters. Term 6 represents the trend in DHW attributed to RSLR at each respective gauge, where t is time (days). An additional term was initially added to the model to test the influence of local wind speed and direction on driving DHW setup. However, after testing various configurations of this term, it was found that the NTR term already accounts for a majority of the non-tidal, non-fluvial forcing. This is likely due to the orientation of the major estuary axis matching the coastline, which causes difficulty in differentiating between the wind stress over the estuary and the Ekman-driven wind transport on the open coast. Thus, this term was removed from the model (see supplemental material for more information).

Daily mean values for river discharge and NTR are used in the regression analysis to represent the subtidal processes that occur on daily timescales (e.g., Dykstra & Dzwonkowski, 2020; Dykstra et al., 2024b). We follow earlier versions of the model, which have similarly used mean daily values to predict HHW and LLW (e.g., Jay et al., 2011, 2016). Using daily maximum values for NTR and river discharge did not improve, and in some cases reduced, model skill. See supplemental materials for more information.

The coefficients a_0 to a_5 in Eq. 1 are found by robust linear regression at both the Georgetown and Conway stations. Initially, exponents are set as: $n1w = 0.6$, $n1p = 0.6$, $n2 = 2$ and $n3 = 1.5$ based on theoretical values following Kukulka and Jay (2003). Exponents are then analyzed through an iterative process where the theoretical ranges from Jay et al. (2016) are tested for each exponent at each station. Starting exponent values are selected within the theoretical ranges; however, the starting values did not significantly impact the final values after iterative testing. A resulting exponent combination is chosen based on the model run with the lowest root mean square error (RMSE). 95% confidence intervals are calculated for each coefficient based on standard errors output calculated using the Matlab function *robustfit*. The optimized exponents and coefficients, along with the associated error ranges, are used with median forcing values of daily river discharge, tidal range, and NTR to calculate contributions to DHW at each station under these conditions. At each station, a time series of each term in Eq. 1 is generated using the calculated coefficients and exponents with time series of T, Q, and NTR. The coefficient of determination (R^2) and RMSE are calculated for each station to evaluate model fit and average error. Calculated coefficients and the associated confidence intervals are reported in the supplemental materials.

Flood Days Determination

To evaluate how various water level forcing mechanisms (see Eq. 1) influence minor 'nuisance' flooding, we define flood thresholds for two Lower Winyah communities: 0.88 m NAVD88 at the Georgetown Pee Dee River station, and 1.48 m NAVD88 at the Conway Waccamaw River station. The thresholds are established by surveying flood events in the communities near the gauges, ensuring meaningful comparison between modeled water levels and impact. An RTK-GPS elevation survey is used to deduce a minor flood threshold for Georgetown, while photographs of minor flooding compared with the local USGS gauge measurements are used to deduce a minor threshold

for Conway. A moderate flood threshold is also established for each station by increasing the elevation of the minor flood threshold by 30 cm, following Sweet et al. (2018). Using this approach, the moderate flood threshold is 1.18 m NAVD88 for Georgetown and 1.78 m NAVD88 for Conway. For more information about how the flood thresholds were established, see the supplemental material.

Flood days are identified as any day when DHW exceeds the flood threshold at the Georgetown and Conway gauges from 2017 to 2024 (e.g., Sweet et al., 2021; McKeon & Piecuch, 2025). The frequency of daily flooding calculated from the modeled and measured DHW time series are compared as a measure of model error. For each day that the modeled DHW exceeds the flood threshold, the day is classified as either a single-mechanism flood day or a compound flood day (depending on whether only one forcing mechanism or multiple mechanisms causes DHW to exceed the minor flood threshold). These flood days are analyzed for seasonal to multiannual trends and variability, as well as compared spatially between stations. The following section describes how the contribution of each forcing mechanism to the total water level is determined.

Forcing Mechanism Contribution to DHW

We assess the relative contributions of each forcing mechanism to modeled DHW level using our regression model, particularly during water levels that exceed local flood thresholds. Effectively, we produce a time series of each term in Eq. 1, utilizing the forcing data and the model coefficients and exponents for each station. For example, the NTR contribution to total modeled DHW is calculated as, $C_{Contrib} = a_4 C(t)$. Adjusted DHW (referred to as DHW_{adj}), is calculated by subtracting the vertical offset (term 1 in Eq. 1) and long-term trend (term 6 in Eq. 1) so that the remaining variability in DHW is due to the combination of river discharge, tides, and NTR. The percent contribution of each forcing mechanism to DHW_{adj} is calculated as a time series for total river discharge, tides and NTR. The contribution of combined river discharge of the Waccamaw and Pee Dee River is calculated as $R_{pc} = \frac{a_1 Q_{Waccamaw}^{n1w} + a_2 Q_{Pee\ Dee}^{n1p}}{DHW_{adj}}$. The contribution of tides is calculated as $T_{pc} = \frac{a_3 T^{n2} Q_{pw}{}^{-n3}}{DHW_{adj}}$ The percent contribution of NTR is calculated as $C_{pc} = \frac{a_4 C(t)}{DHW_{adj}}$ and $R_{pc} + T_{p\ c+}\ C_{pc} = 100\%$ for each modeled DHW. Some forcing mechanisms, such as NTR, can sometimes lower DHW. As a result, percent contributions of other forcing mechanisms (such as discharge) may occasionally exceed 100%. For example, if the adjusted water level was 0.18 m, the contribution of total discharge could be R_{pc}= 150% (0.27/0.18), the contribution of tides, T_{pc}= 50% (0.09/0.18) and C_{pc}= −100% (−0.18/0.18). While other studies, such as Li et al. (2022) have chosen to represent the individual components as less than 100%, the results can be interpreted and compared similarly. The percent contribution of each forcing mechanism is used later to assess their relative importance at each water level station. Summary statistics, including 25th and 75th percentiles, are calculated for the percent contribution of each forcing mechanism and reported for each station. To account for model error, the lower and upper confidence intervals for the coefficients are used to generate two additional time series of low and high estimates of the contribution of each forcing mechanism during the flood days. The associated ranges of contributions are reported in the results.

Future Changes in Flood Frequency Due to RSLR and Changes in Discharge

We investigate future change in flood frequency at Conway and Georgetown under two possible RSLR rates and future river discharge conditions. We calculate future time series of modeled DHW over the time period from July 21, 2034 to May 21, 2041 (matching the original time series length) under four scenarios, then calculate the number of future flooding days for each case. We choose this near-term future time period because changes in flood frequency farther in the future are likely to be dominated by the acceleration in global SLR.

The four scenarios are as follows (Table 2): (i) a “low” RSLR rate with no future change in river discharge; (ii) a low RSLR rate with a 10% increase in discharge; (iii) a “high”

Table 2 The four future scenarios with varying RSLR and river discharge to simulate possible future changes in flood frequency for Conway and Georgetown

Scenario	RSLR Rate	Discharge Change
Scenario i	low	no change
Scenario ii	high	10% increase in discharge
Scenario iii	low	no change
Scenario iv	high	10% increase in discharge

RSLR rate with no change in discharge; and (iv) a high RSLR rate with a 10% increase in discharge. The low RSLR rate (3.4 mm/yr) is the long-term historical measured rate at the NOAA Springmaid Pier station from 1957 to 2024. The high RSLR rate (11 ± 1.7 mm/yr at Georgetown and 14 ± 1.9 mm/yr at Conway) is the regression-based RSLR rate calculated at each station over the 2017–2024 period (coefficient a_5 in Eq. 1) and includes a recent acceleration in SLR caused by changes in oceanic circulation (Dangendorf et al., 2023) and spatially varying VLM that increases local RSLR at both stations. Section 4 of the Supplement provides a detailed explanation of calculation of the four future DHW time series, but in brief, we use the a_1 to a_4 coefficients and exponents ($n1w$, $n1p, n2$ and $n3$) calculated for the 2017–2024 historical time period (Eq. 1), adjust the starting sea level to the year 2034 (a_0 term), and set the a_5 term to the low or high RSLR rate. We use 2017–2024 observed tides, NTR, and discharge (with a 10% increase applied for scenarios ii and iv). The use of historical tides is reasonable because initial testing indicated that interannual tidal variability has a small impact (1–2 cm) on water level at Georgetown and Conway. This variability is negligible compared to the range between the low and high RSLR scenarios.

Results

Model Performance

The physics-based regression model (Eq. 1) reproduced water levels driven by river discharge, tides, and NTR (Fig. 3). Adjusted R^2 values range from 0.95 for the Conway River station to 0.71 for the Georgetown Station. Model RMSE is 0.11 m at the Conway station and 0.08 m at the Georgetown station. Georgetown's lower RMSE and adjusted R^2 values result from its smaller dynamic water level range and greater modeling uncertainty. This uncertainty is caused by unresolved, sub-daily processes (e.g., local wind and waves) that the model does not include. Conversely, at the fluvial-dominated Conway station, DHW levels are primarily controlled by river discharge; thus, the RMSE is slightly higher due to the greater magnitude variability in water levels compared to the downstream station (DHW absolute range of ~5 m at Conway station compared to 1 m at the Georgetown Station). The model had the largest error during extreme high water level events, such as Hurricane Florence in September 2018 (Fig. 3; grey shaded box).

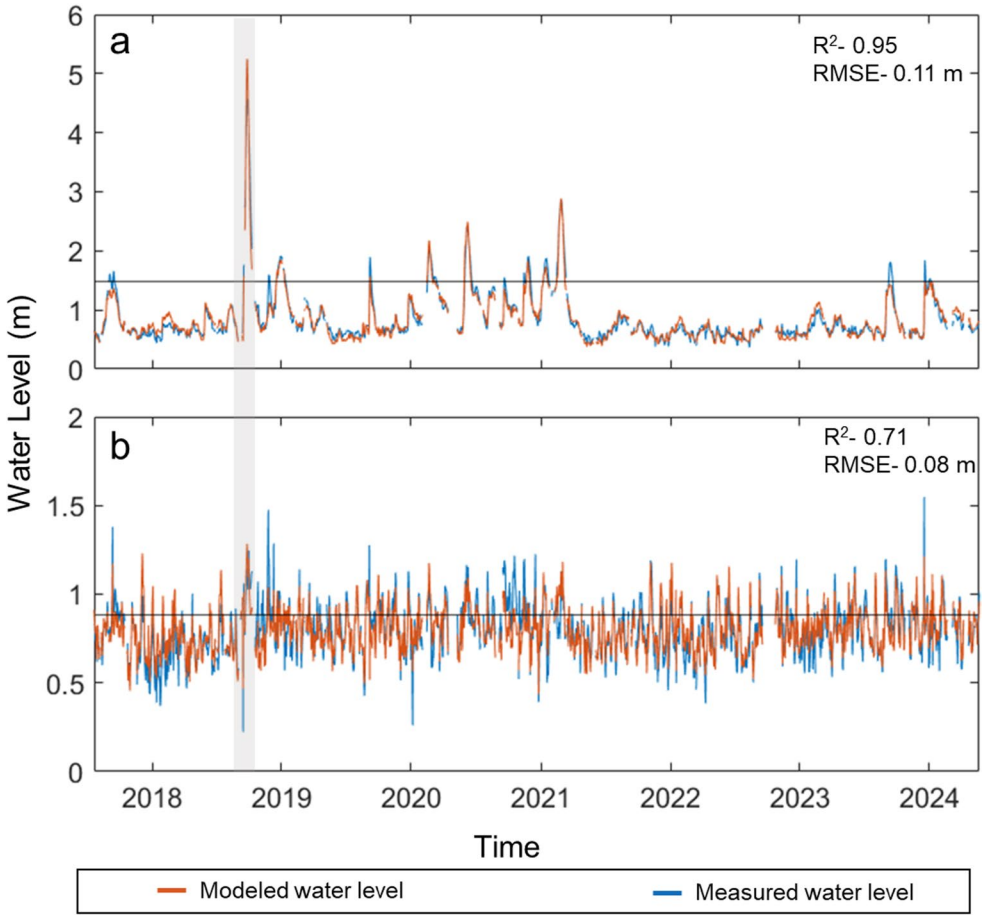

Fig. 3 Modeled and measured DHW at Conway station (**a**) and Georgetown station (**b**). Orange denotes the modeled water level, and blue represents the measured water level. The black line in both panels represents the minor flood threshold established at each station

Spatial Variability of Processes Controlling DHW

Tides and river discharge have similar impacts on DHW at Georgetown under median forcing conditions, while NTR contributes slightly less and can also cause lower mDHW values (Fig. 4a). Median contributions from all water level drivers at Georgetown are: 14 ± 0.6 cm from tides, 10 ± 1.1 cm from Pee Dee River discharge, 10 ± 0.4 cm from NTR and 6 ± 0.7 cm from Waccamaw River discharge. The typical variation in water level (Fig. 4a) and percent contribution to a flood day (Fig. 4c) produced by each forcing mechanisms is shown by boxes, and span the 25th to 75th percentile contributions (discussed more in *FORCING MECHANISM CONTRIBUTION TO DHW*). Using this measure, the contribution of each type of forcing mechanism to mDHW varies through a range of 20–25%, around a different baseline. Combined river discharge (Waccamaw + Pee Dee) contributes 29–54% to DHW_{adj}, while tides contribute 23–51%, and NTR contributes 9–31% (Fig. 4). At Georgetown, the rate of RSLR over the 2017–2024 period of analysis is estimated to be 11 ± 1.7 mm/yr, consistent with high RSLR rates of > 10 mm/yr along the Southeastern coast of the US since 2010 (Dangendorf et al., 2023).

For the Conway station, river discharge contributes most significantly to high-water events (i.e., mDHW), with tides and NTR a minor or negligible facto (Fig. 4b and d). Outlier values shown in Fig. 4b discharge occurred during Hurricane Florence in 2018.Contributions to DHW under median forcing conditions are: 34 ± 0.5 cm from the Waccamaw River, 30 ± 1.5 cm from the Pee Dee River, 11 ± 0.7 cm from tides, and 5 ± 0.4 cm from NTR. Again, examining 25th to 75th percentile contributions of each forcing mechanism reveals that combined river discharge contributes 65–89% to DHW_{adj}, while tides contribute 6–28% and NTR contributes 2–9% to DHW_{adj} (Fig. 4). The estimated RSLR over the period of analysis from 2017 to 2024 is 14 ± 1.9 mm/yr.

Flood Days

In Georgetown, 623 measured high waters exceed the minor flood threshold elevation (0.88 m NAVD88) from 2017 to 2024. Similarly, 534 high waters in the modeled DHW time series exceed the same threshold. Of the 534 modeled flood days, 79% (422 flood days) correspond to measured flood days. Most of the remainder were flood days that nearly exceed the threshold in the measured record. Only 8 of the 534 flood days (~ 1 flood day/year on average) reach the moderate flood threshold of 1.18 m NAVD88. Combined Waccamaw and Pee Dee River discharge is the primary driver of 30–35% (162–186) of the modeled flood days. Tides are the primary driver of 44–46% of (237–244) flood days, and NTR of 21–24% of (111–128) flood days. Here, the range of flood days is determined by calculating contributions using the 95% confidence interval of model

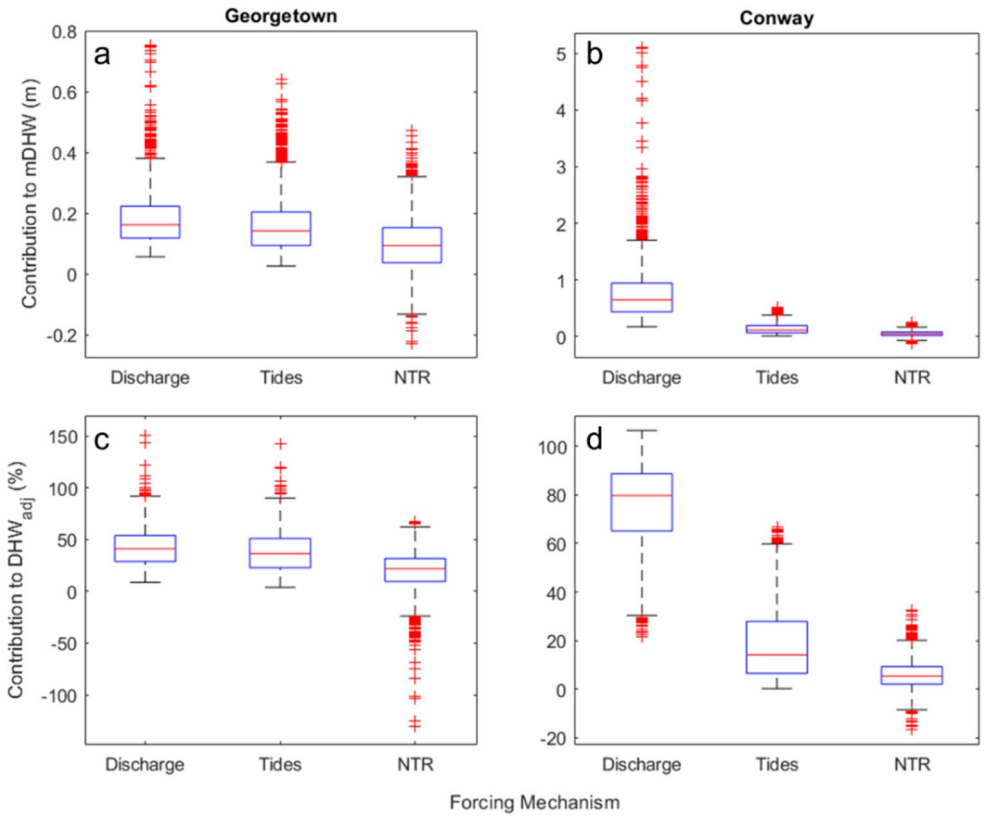

Fig. 4 Statistical distribution of forcing mechanisms contribution (river discharge, tides and NTR) to modeled DHW (mDHW) in meters as well as percent contribution to DHW_{adj} at the Georgetown (**a** and **c**) and Conway (**b** and **d**) stations. Box indicates the 25th and 75th percentiles, the whiskers extend to the non-outlier maximums and minimums and the "+" indicates outlier values

coefficients. Both tides and river flow can dominate a flood day, or have a nearly negligible influence, depending on their relative forcing. Thus, tides contribute a range of 4–97% to DHW_{adj}, and combined river discharge contributes 9–95% to DHW_{adj} during flood days (Fig. 5). When river discharge is low, tidal influence can be high. Due to the frictional relationship between river discharge and tides, as river flow increases the tidal contribution to DHW_{adj} is lowered, leading to a high range of contributions in both of these mechanisms. NTR contributes − 12–67% during flood days, where negative contributions indicate NTR lowering total water level.

During the period of analysis at the Georgetown station, only 2–10% of the modeled flood days (10–53 flood days), are classified as single-mechanism flood days, where only one forcing mechanism causes DHW to exceed the minor flood threshold. Tides are the singular forcing mechanism for 1–4% of the modeled flood days (2–18 flood days) and combined river discharge for 2–7% (8–34 flood days). NTR only produces one single-mechanism flood day using the upper range of the uncertainty in the model coefficient for the forcing. Compound events account for 90–98% of modeled minor flood threshold exceedances at the Georgetown station (481–524 flood days). Tides are the most impactful forcing mechanism for increasing DHW; meaning, the tidal contribution has the highest value compared to the riverine and coastal contributions during most modeled flood days. This occurs during 41–45% of total modeled flood days (219–242), followed by combined river discharge, which causes the larger water level contribution in 29–30% of the total modeled flood days (152–162). Finally, NTR is the most prominent forcing mechanism in 20–24% of total modeled flood days (110–128).

Upstream at the Conway Waccamaw River station, 192 flood days in the measured DHW record exceeded the minor flood threshold of 1.48 m NAVD88. Within the modeled record, 128 flood days are identified. Nearly all the modeled flood days align with measured flood days (123 out of 128). Seventy-one (71) of 128 flood days reach the moderate flood threshold of 1.78 m NAVD88 (~10 flood days/year on average). A majority of the 128 flood days (75–95%; ranging from 96 to 122 flood days) are single-mechanism floods driven by river discharge. However, during the remaining compound floods, the influence of NTR and combined river discharge is responsible for 5–11% of the total modeled flood days (6–14). Overall, the combined river discharge contributes 86–101%, tides contribute 0–4%, and NTR contributes − 4–11% (Fig. 5). The higher than 100% contribution of river discharge occurs when a negative NTR lowers water levels. Since river discharge is the primary driver of flood days at the Conway station, several flood days are often the result of the same single fluvial event.

The variability of flood days closely aligns with the driving forcing mechanisms at both the Georgetown and Conway stations (Fig. 6). River-dominated flooding occurs consistently during periods when the monthly average combined river discharge exceeds ~350 m/s, specifically across three timeframes (Aug. 2018- May 2019; Dec. 2019- Apr. 2021; Dec. 2023- Apr. 2024). Although monthly tidal range variability is small (~1.5–1.8 m), tidally driven flood days are most frequent from June to December, particularly when river discharge is low. NTR averages show no clear monthly trend,

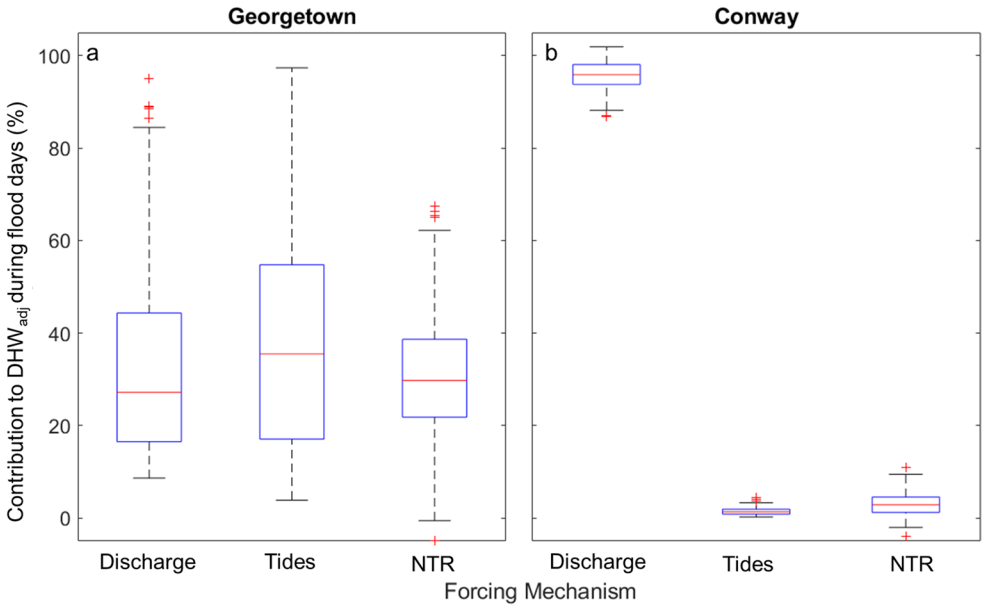

Fig. 5 Percent contribution of forcing mechanism to DHW_{adj} during flood days for the Georgetown (**a**) and Conway (**b**) stations. Box indicates the 25th and 75th percentiles, the whiskers extend to the non-outlier maximums and minimums and the "+" indicates outlier values

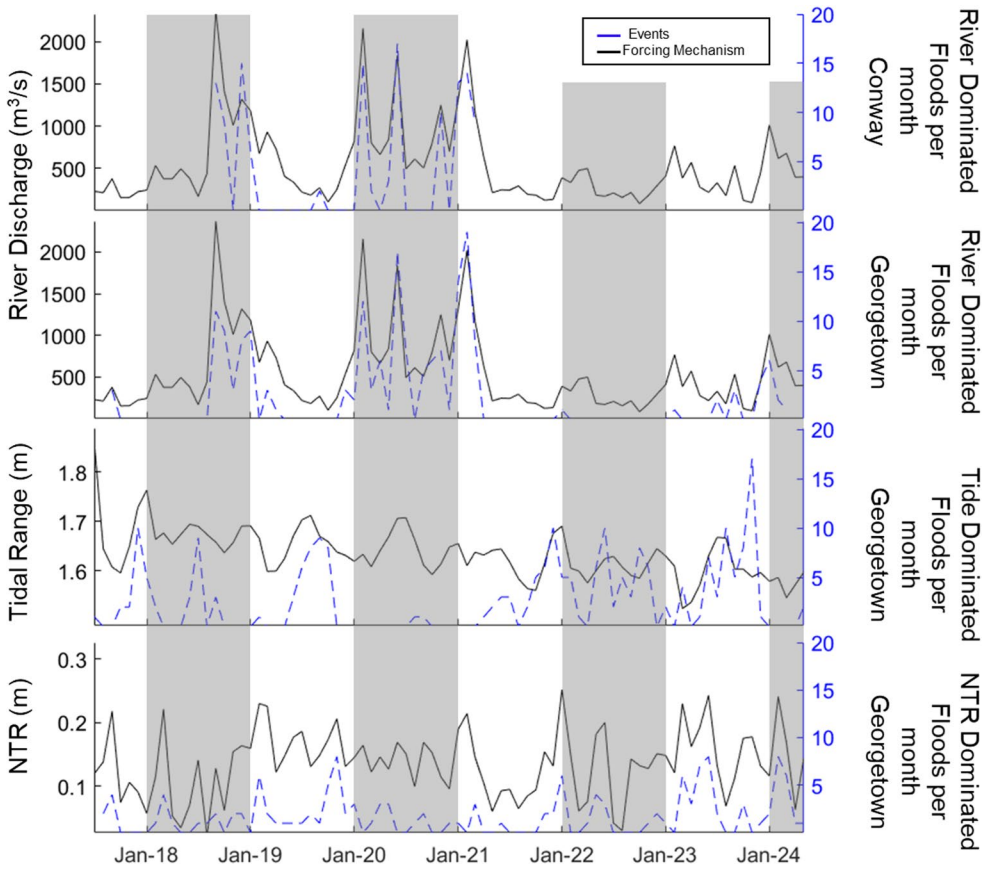

Fig. 6 Flood drivers (black) and the number of flood days dominated by each driver (blue). Flood drivers are shown using a monthly mean magnitude. Note that Conway only appears in the first panel due to river discharge being the only dominant forcing mechanism at this station

which is reflected in the counts of NTR-driven flood days as well. In part, this is a consequence of ascribing most seasonal variation to the SA and SSA tidal constituents; hence, a significant seasonal variation in tidally-produced flooding is modeled at Georgetown (Fig. 6c). Attributing most of SA and SSA to the NTR would slightly change attribution statistics, particularly seasonally; however, without detailed numerical modeling, there is no way to decompose the astronomic from NTR contribution to seasonal tides. Nonetheless, since both tidal and NTR both stem from the ocean, their sum provides an assessment of the combined coastal influence (Fig. 6c and d). Overall, the Georgetown station's annual flood days varied from 64−99 (with a peak in 2023), while Conway's flooding was concentrated between 2018−2021. The Conway station's subsequent lack of flood days after 2021 corresponds directly to a sustained period of lower river discharge in the Pee Dee and Waccamaw systems.

Impact of Relative Sea Level Rise (RSLR) on Flood Day Frequency

The four future time series of DHW from 2034 to 2041 indicate how a continued rise in RSL along with a 10% increase in river discharge can increase flood frequency over the coming decade when compared to our minor flood thresholds at Conway and Georgetown (Fig. 7). Even applying the lower long-term rate of RSLR from 2034 to 2041 (3.4 mm/year; Scenario i, Table 3), the Georgetown station experiences 1280 flood days over a future 7-year period (140% increase compared to 2017–2024). Adding increased river discharge to this low RSLR scenario (Scenario ii) causes only a slight growth in the number of flood days, to 1301 floods (144% increase compared to 2017–2024). However, extending the higher modern rate of RSLR into the future (11.3 mm/year; Scenario iii), the number of floods surges to 1859 (a 248% increase compared to 2017–2024). Finally, combining high RSLR with increased river discharge (Scenario iv) results in a comparable 1860 flood days (a 249% increase compared to 2017–2024). This equates to flood days occurring on 75% of the days considered, or an average of 216 days/yr. Moderate flooding occurs during 8 out of the 534 modeled flood days during the historical period, and it increases to 58 flood days (Scenario i) and to 183 flood days (Scenario iii) over 2034–2041.

Long-term RSLR rates (Scenario i) increase the number of projected flood days from 128 (2017–2024) to 198 (2034–2041) for the Conway station (55% increase). Under low rates of RSLR and increased river discharge (Scenario

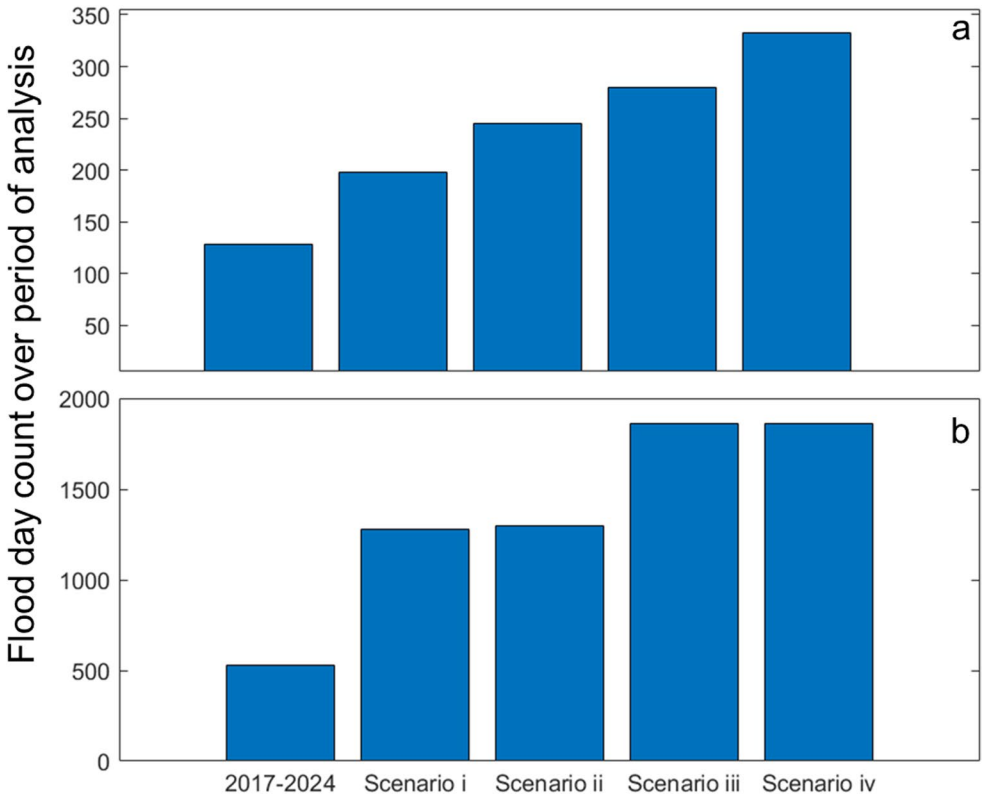

Fig. 7 Flood days for the modeled time period (2017–2024) as well as for the four future scenarios (i-iv) for 2034–2041. The flood days are separated by season for Conway (**a**) and Georgetown (**b**). Note that the y-axis has two different scales. The first bar shows the modeled flood days from the analysis period 2017–2024

Table 3 Rates of RSLR for the two water level stations. The low RSLR (Scenarios i and ii) were estimated based on the historic rate measured at springmaid Pier. The high RSLR (Scenarios Iii and iv) were calculated by applying the rate of RSLR extracted from our regression model

	Conway			Georgetown		
	SLR rate (mm/year)	2024-2034 SLR (mm)	2034-2041 SLR (mm)	SLR rate (mm/year)	2024-2034 SLR (mm)	2034-2041 SLR (mm)
Scenarios i and ii	3.4	34	23	3.4	34	23
Scenarios iii and iv	14.4	146	99	11.3	115	77

ii), this number increases to 245 (91% increase). Under high RSLR (14.4 mm/year; Scenario iii), the number of flood days increases to 280 (119% increase). Finally, under a continued modern rate of RSLR and increased discharge (Scenario iv), the number of flood days increases to 333 (13% of the days considered) which is equivalent to an average of 49 flood days per year (Fig. 7). Moderate flood days increase in frequency to 103–117 (Scenarios i and iii) flood days for Conway over the projected period, compared to 71 from 2017 to 2024.

Discussion

Spatial Variability of Forcing Mechanisms

Consistent with McKeon & Pieuch (2025), this study confirms that compound minor flooding is a widespread and highly variable phenomenon in tidal rivers and estuarine environments. McKeon & Pieuch (2025) found that 55–79% of total flood days over 22 years in the Delaware River Estuary are driven by more than one forcing mechanism.

Our results show that in the lower reaches of the Winyah system, compound floods account for 90–98% of flood days in Georgetown. Upstream, compound floods account for 5–25% of total flood days recorded in Conway. The spatial variability in controlling mechanisms demonstrates consistent patterns in Winyah Bay and the Delaware River Estuary, with tides contributing to more flood days in the lower reaches of the systems and river discharge predominantly driving upstream floods. However, in both systems, river discharge remains an impactful factor in downstream flooding. River discharge was the primary contributor to 33% of all modeled flood days at the Georgetown station and was the predominant driver of single-mechanism floods (64% of single-mechanism floods). River discharge was shown to contribute towards compound flooding in the lower estuary in the Delaware estuary as well, with contributions ranging from 1% ± 1% at Brandywine Shoal to 21% ± 5% at Marcus Hook.

In addition to the physical drivers, the geometry of the system and the topography of the land are important factors in determining flood susceptibility. A study by Feng et al. (2022) comparing the Susquehanna River (Chesapeake Bay) and the Delaware River demonstrated that narrow, low-gradient estuaries on the coastal plain with significant river discharge are more susceptible to compound flooding from the interaction of fluvial input and coastal processes (like storm surge and sea level rise). The Susquehanna system, with its relatively steep gradient and ocean-like receiving water body, shows little fluvial-coastal interaction. Conversely, systems like the Delaware and Winyah are narrow and low-gradient, allowing tides and non-tidal residuals (NTR) to propagate further upstream, increasing interaction. In the Winyah system, an interconnected network of narrow channels further enhances this interaction. These comparative studies highlight significant spatial variability in flood hazard applicable to estuarine analysis, despite differences in forcing magnitude (tidal range and river discharge) and geometry between systems like the Delaware and Winyah.

For the upstream Conway station, river discharge is the most influential forcing mechanism causing flood days. However, NTR and tides contribute to flood threshold exceedences for 13% of measured flood days. The rate of RSLR for the Conway station is also slightly higher than for the Georgetown station (14.4 ± 1.9 compared to 11.3 ± 1.7 mm/yr), though the confidence intervals overlap. Both rates are higher than the coastal rate of DHW increase of 8.6 mm/yr (2017–2024) estimated at the Springmaid Pier. Baranes et al. (2023) showed that 30 of the 41 stations analyzed along the tidal rivers of the Sacramento-San Joaquin Delta in California exceeded both the global rate of RSLR and the coastal rate of RSLR. The spatial variability in RSLR was attributed to variations in vertical land motion (Baranes et al., 2023). In the Lower Winyah watershed, GNSS stations show rates of vertical land motion ranging from 0.37 ± 0.83 to −14.94 ± 3.5 mm/yr, which could explain the spatial differences between the two river stations and the coastal RSLR trend (Blewitt et al., 2018). These rates are much higher than the satellite-measured global average SLR over the same period (4.0 mm/yr) (Beckley et al., 2024). Additionally, ocean circulation and climatic cycles are likely driving an anomalously high RSLR in the southeastern United States, with rates exceeding 10 mm/yr from 2010 to 2022 (Dangendorf et al., 2023; Yin, 2023). Thus, regional oceanic factors also help explain the high RSLR estimated at the Springmaid Pier and within the Winyah Bay estuary, in addition to large and variable rates of VLM.

The influence of RSLR and coastal processes on inland flooding far from the coast (here, ~90 km) is rarely considered but deserves more attention, given predictions of future sea-level rise (e.g., Hamlington et al., 2022) and observations of large vertical land motion rates and variability in other estuarine regions (e.g., Baranes et al., 2023). Here, we use the regression-derived RSLR rates to show that coastal processes will likely increasingly impact upstream reaches of the estuary in the future. Nonetheless, it remains unclear how to partition observed RSLR in the estuary among coastal rise, vertical land motion, and hydrodynamic feedback effects, which can lower mean water levels (e.g., Jay et al., 2011; Ralston et al., 2019; Talke et al., 2021).

Studies suggest that the effects of sea-level rise diminish with increasing river flow, especially further inland (e.g., Helaire et al., 2020; Orton et al., 2020). For example, Orton et al. (2020) observed a linear increase in flood hazard due to RSLR in the lower and middle Hudson River (within ~113 km of the coast). However, farther upstream near Albany (~220 km from the Hudson's mouth), increased sea-level produced a lessor impact, and flood risk decreased by 30–60% due to the greater influence of river flow. Compared to Albany (220 km on Hudson River), Conway is closer to the estuary mouth (91 km) and has a lower surface river slope (2 mm/km compared to Albany's 5.6 mm/km). RSLR may therefore impact Conway flood hazard similarly to lower and middle Hudson River stations. If this is the case, it would suggest that sea-level rise is transmitted to Georgetown and Conway with little or no attenuation. The NTR model coefficient (a_4 in Eq. 1) provides insight into how daily-timescale fluctuations in coastal sea level are attenuated at inland stations. For example, the coefficient values of 0.76 at Georgetown and 0.45 at Conway indicate that a 1 cm positive NTR would raise DHW by 7.6 mm at Georgetown and 4.5 mm at Conway. However, a more detailed numerical modeling analysis would be required to determine whether the inland attenuation of daily-timescale coastal ocean variability matches that of longer-timescale

SLR (e.g., Kumbier et al., 2018; Ralston et al., 2019; Helaire et al., 2020; Orton et al., 2020; Talke et al., 2021). As such, it remains uncertain how a given increment of coastal sea level rise translates into an increase in DHW in the inland areas. Nonetheless, our study demonstrates the need to consider RSLR in decision-making and community adaptation planning, even in locations far from the coast that are dominated by river-flow-driven floods.

Flood Threshold Comparison

This study defines minor flood thresholds based on community observations of water levels that lead to flooding. With these impact-based thresholds at Conway and Georgetown, flood days occur significantly more frequently than reported by studies that use empirically derived thresholds. NOAA has developed empirical minor, moderate, and major flood thresholds as a function of greater diurnal tide range (GT) by regressing available impact-based thresholds against the great diurnal range, GT (Sweet et al., 2018). Using the difference between mean DHW and DLW to approximate GT, we calculate empirical minor flood thresholds for Georgetown (1.35 m NAVD88) and Conway (1.36 m NAVD88) based on the methods in this study. Using this empirical threshold, we find just 3 flood days in the measured record at Georgetown and 0 flood days in the modeled record during the same time period as our analysis. Using the calculated empirical threshold for Conway, we find 258 minor flood days in the measured record and 188 in the modeled record. Thus, empirical thresholds overestimate flood days in the upstream part of the system, while severely underestimating flood frequency in downstream reaches. While empirical thresholds are essential for regional minor flooding studies and characterizing the chronic nature of flooding related to rising RSLR, impact-based thresholds hold greater value at a local scale, especially for low-lying communities like Georgetown. Additionally, the empirical thresholds inadequately incorporate river flow effects on water level, and may therefore become increasingly inappropriate in upstream reaches influenced by compound minor flooding (e.g., Conway).

At Springmaid Pier, the nearest coastal NOAA tide gauge, the empirical minor flood threshold is 1.31 m NAVD88. Utilizing this empirical threshold, 54 minor flood days occurred at Springmaid Pier from 2017 to 2024. Utilizing the NWS impact-based threshold (1.17 m NAVD88), 216 flood days occurred during the same period. Piecuch et al. (2025) used a nonparametric statistical analysis of impact-based flood data and defined a minor flood as Springmaid Pier of 1.16 m NAVD88. This threshold identified 247 flood days during our analysis period. Thus, using the empirically-derived threshold also produces an undercount at the Springmaid Pier. Additionally, this analysis shows that the lower estuary (e.g., Georgetown) experienced many more minor floods than Springmaid pier (534 vs. 216), and has a higher overall flood risk.

While research on the increased frequency of minor flood days is extensive, the concept of chronic flooding, where all flood impact levels (minor, moderate, and major) are increasing in frequency due to RSLR, is a developing area of study (see Thompson et al., 2019; Hague et al., 2023; Hague & Talke, 2024). Both the estuarine stations as well as Springmaid Pier already experience chronic flooding (> 50 days per year). Our results also suggest that the number of moderate floods (30 cm above the minor flood level) is rising. Projections utilizing the historical long-term rate of RSLR (1957–2024) for the future period from 2034 to 2041 result in 10 moderate flood days per year at the Georgetown station and 15 flood days/year at the Conway station. Applying the more recent RSLR (2017–2024) would result in 26 and 17 moderate flood days per year at Georgetown and Conway, respectively. We also note that while our methodology provides estimates of the number of flood days, the daily resolution of our modeled time series prevents us from determining duration and impact.

Physical and Economic Impacts of Flooding

Our study focuses on future changes in exceedances of an impact-based flood threshold over the next several decades. Economic consequences are a function of inundation depth and duration of flooding. While minor flooding causes less damage per event than extreme events, the higher frequency and cumulative duration may lead to greater damage over time (Moftakhari et al., 2017). However, the impact of each of these flood events will vary. First, the spatial extent of flooding will vary depending on the mix of forcing factors. Large spring tides are most influential close to the coast, whereas river flooding is more important upstream. Moreover, coastal topography varies by location. Therefore, the spatial footprint (and thus the impact) of each event is likely different. Flood duration can be determined by the depth of flooding, tidal properties, fluvial characteristics, runoff, and groundwater impacts (Rahimi et al., 2020; Talke, 2025). For a community like Georgetown, this means that, where NTR, tides and discharge all play influential roles in the production of flood events, the duration of flooding can be variable, lasting anywhere from a few hours to multiple days, depending on which mechanisms are contributing to the high-water levels. In contrast, in Conway, where river discharge is the primary driver of flood events, flood waters last days to weeks as high river flow events dampen the influence of tides and cause persistently high-water levels (Pietrafesa et al., 2019; Gori, Lin, and Smith, 2020; Talke et al., 2021).

Flood durations will likely increase non-linearly due to both RSLR and tidal properties (Talke, 2025). Municipalities can use techniques such as the regression model employed in this study to predict the impact of potential high-discharge events or even the compounding of multiple mechanisms on their communities.

The challenges facing Georgetown and Conway are microcosms of many low-lying inland communities influenced by both coastal and fluvial processes. Case studies have demonstrated that minor flooding increases traffic delays and roadway repair costs. However, Fant et al. (2021) showed that with adaptation and protection measures, Charleston County may be able to reduce traffic delays caused by flooding by 91% by 2050. Communities along tidal rivers, such as the Waccamaw and Pee Dee systems, could implement similar measures to Charleston by incorporating future SLR scenarios and flood hazard analysis into budgeting and land planning. Our study provides this region with locally relevant RSLR rates that are useful for hazard analysis and future planning in the Lower Winyah watershed. Recently, there has been a decline in industrial activities in Georgetown, with the community shifting its economic goals towards growing tourism and a hospitality focus for the city (Georgetown County, 2024). A majority of the shops and restaurants are located near the water and already experience flooding. An increase in minor flood frequency would hinder visitor traffic with the potential to impede economic growth in these sectors. Hino et al. (2019) studied the economic impact of high-tide flooding in the historic downtown of Annapolis, Maryland. They showed that in 2017, downtown businesses lost $86,00-$172,000 (0.7–1.4%) of their annual revenue due to reduced visits during flood events. They estimate that with an additional 8–30 centimeters of RSLR, downtown visits could be reduced by as much as 24%. Here, we suggest that compound minor flooding may produce similar disruptions far from the coast, and that communities such as Georgetown and Conway should consider evolving flood risk and the results of this study to develop plans to mitigate future economic risks.

Study Limitations

The goal of this study was to provide first-order insights into the flood mechanisms of the Lower Winyah Watershed, but the current regression approach necessarily omits several important flood-generating processes, including local wind, pluvial flooding, storm water backups, nonlinear sea-level rise/vertical land motion, and groundwater effects (Rahimi et al., 2020; Leijnse et al., 2021; Oelsmann et al., 2024). Future efforts to improve the model should also consider other nonlinear interactions beyond the river-tide dynamics accounted for here, specifically storm surge-tide interactions (Xiao et al., 2021). Furthermore, since this study examined only DHW, multiple flood events occurring on the same day were not resolved. As this study provides first-order insights into flood mechanisms in the Lower Winyah Watershed, various methodological aspects could be improved to gain a deeper understanding of the dynamics. On long time scales, river discharge and atmospheric forcing from distant and regional sources can alter circulation patters (e.g., Gulf Stream) and cause water levels to deviate from our harmonic representation with SA and SAA, which could underpredict the NTR seasonality and overpredict tidal seasonality (Noble & Gelfenbaum, 1992; Piecuch et al., 2018). Further work could be done to decompose the coastal seasonal cycle into tidal and nontidal components. On shorter time scales, future studies could improve the temporal resolution of the model by incorporating high-frequency (hourly) river flow and storm surge data into flood estimates and account for the time lags between ocean and river forcing (e.g., Dykstra et al., 2022; Jay et al., 2016). Additional dynamics associated with low lying rivers (e.g., flow hysteresis) and small watersheds (e.g., flashiness) could be investigated with different regression coefficients for fast changing or slow changing river flow events and the river rising or falling limbs.

Small uncertainty and spatial variation in measurements of forcing processes (tides, NTR, river flow), along with ungauged processes (e.g., small creeks), may drive additional (but small) errors and the estimated RMSE of 0.10 m for Conway and 0.08 m for Georgetown. Combined with uncertainty in our coefficients, only approximately 66% of actual flood days between 2017 and 2024 are modeled by our approach. Thus, improvements in modeling and monitoring are needed to help communities fully assess/predict the minor flood problem and devise solutions. Further capturing the timing and duration of flood events requires two specific efforts. First, there is a need for a denser monitoring network, particularly on ungauged tributaries along the estuary. Second, more detailed modeling is necessary to address the hydrodynamic complexities of the low-elevation, anastomosing nature of the coastal rivers in this area. Nonetheless, our approach captures the most important processes driving minor floods.

Finally, this study demonstrates the importance of high-spatial resolution multi-year records of water level and physical forcing mechanisms. Our study time frame was limited by the short length of the water level time series for the Georgetown USGS station, which began collecting high-resolution water level data in 2017. While there has historically also been a spatial gap in water level data along the tidal rivers and surrounding estuaries in the Lower Winyah Watershed, organizations such as Southeast Coastal Ocean Observing Regional Association (SECOORA) have recently installed several gauges, including within Winyah

Bay. Utilizing this data in a future analysis will give a more complete picture of the spatial gradient in forcing mechanisms and better inform the communities in this region in regards to the relative importance of factors that lead to high water levels and flooding.

While the time series analyzed here was relatively short, we conducted a series of sensitivity tests in order to characterize how robust the results are over various time frames. Since the Conway station has a longer time series, we reran the model with data from 2015 to 2025 at this station. We found that the coefficients and exponents, as well as model fit and error, were nearly identical to those from the time period used in the analysis presented here. The rate of DHW increase at Conway from 2015 to 2025 was 13.5 ± 1.0 mm/yr, which is just slightly lower than the 14.4 ± 1.9 mm/yr calculated for the period between 2017 and 2024. This linear trend, calculated using the regression model, is, however, sensitive to starting and ending years. When our analysis was extended from July 2017 to July 2025, rates of DHW rise dropped to 8.5 ± 1.5 mm/yr at the Conway station and 4.7 ± 1.4 mm/yr at the Georgetown station. This change in RSLR also occurs in monthly MSL data from the Springmaid Pier and the Charleston, SC, NOAA coastal stations. RSLR at the Springmaid Pier drops from 15.9 ± 5.5 mm/yr from July 2017- May 2024 (our analysis period) to 8.4 ± 5.0 mm/yr for the July 2017 to July 2025 period. Similar trends are also seen in the change in DHW calculated at Springmaid Pier (Table 4). Thus, the projected evolution of flooding from 2034 to 2041 using 2017–2024 may be overestimated, especially if recent anomalous RSLR along the southeast US Coast relaxes. On the other hand, using the much lower long-term rate (3.4 mm/yr) at the Springmaid Pier likely underestimates near-future trends in flooding. Thus, our estimates of future flood evolution may bound the set of likely future trajectories, all of which show increasing flood frequency over time. Thus, although the specific frequencies of flood events and the relative influence of each driving mechanism might be contingent on available data, the main conclusions about the spatial differences in event drivers and the critical role of compounding mechanisms remain valid.

Table 4 Rates of RSLR (from monthly MSL) and DHW increase at springmaid pier station with 95% confidence intervals for three different periods of time to show the sensitivity of rates to the starting and ending years

Time Period	RSLR Monthly MSL (mm/yr)	DHW increase (mm/yr)
July 21, 2017 to May 21, 2024	15.9 ± 5.5	8.6 ± 4.3
January 1, 2017 to December 31, 2024	18.0 ± 5.4	13.8 ± 3.4
July 1, 2017 to July 1, 2025	8.4 ± 5.0	3.3 ± 3.5

Conclusions

A physics-based regression model was used to determine the spatially varying physical drivers of minor flooding in the Winyah Bay estuary. The results demonstrate the compound nature of floods, particularly in the lower portion of the estuary, where tides, discharge, and NTR all play important roles in driving flood events. We find that empirically-derived flood thresholds overestimate flood frequency in the upper estuary (Conway) and underestimate flood frequency in the lower estuary (Georgetown). We also find that impacts occur at a lower water surface elevation in low-lying communities within the estuary, such as Georgetown, than at the impact-based and empirically-derived flood threshold at a nearby coastal gauge (Myrtle Beach).

We investigated minor, coastally influenced flooding upstream in Conway, 91 rkm upstream of the estuary mouth. Results show that river discharge is the primary driver of high-water levels for 111 out of 128 flood days between 2017 and 2024. Out of these 128 flood days, 71 (55%) of these flood days also exceeded a moderate flood level. Under a future rise in RSLR and an increase in river discharge, flood frequency would increase up to 119% over the next decade. Downstream at the Georgetown station (23 rkm), located near the opening to the Winyah estuary, compound flood days are most common, with significant contributions from high tides, river discharge and NTR. Under even a low RSLR scenario utilizing the measured long-term historic rate of 3.4 mm/yr, flooding in Georgetown is projected to double over the next decade. This is occurring because many tides are already close to the flood threshold, such that the projected local increase in RSLR of 57 mm by 2041 (Table 3) is anticipated to result in an increase in the frequency of high tide flood events.

Our results suggest that municipalities along tidal rivers should consider coastal RSLR, local variations in vertical land motion, and possible changes in river discharge when planning future zoning changes, emergency management, and infrastructure projects. For locations that are already experiencing flooding in the tidal and tidal-fluvial reaches of rivers and have an elevated rate of RSLR, the transition to chronic or near-daily inundation may occur as early as the coming decade. Moreover, inland communities upstream will experience an increase in flooding due to coastal ocean effects. In such communities, RSLR is typically not considered in planning, yet these daily floods will likely cause increased economic and physical damage to local infrastructure if not addressed.

Supplementary Information The online version contains supplementary material available at https://doi.org/10.1007/s12237-026-01672-y.

Acknowledgements This study was supported in part by the South Carolina Department of Natural Resources.

Author Contributions M.F. was responsible for the data collection, analysis, interpretation and initial manuscript development. H.B. was responsible for initial model development as well as support with data interpretation and manuscript development. S.D. was responsible for support with model development, data interpretation and manuscript development. S.T. was responsible for project conception as well as support with data interpretation and manuscript development. T.H. was responsible for project conception as well as support with data interpretation and manuscript development.

Funding Open access funding provided by the Carolinas Consortium.

Declarations

Competing interests The data analyzed in this study are available on the USGS and NOAA websites. Other supporting data related to this study are available from the Corresponding author Madison Fink, upon request. SAT was funded by the Strategic Environmental Research and Development Program, contract W912HQ24C0020. The authors declare that they have no competing interests.

References

Allen, D., Allen, W., Feller, R., & Plunket, J. (2014). *Site Profile of the North Inlet – Winyah Bay National Estuarine Research Reserve*. North Inlet – Winyah Bay National Estuarine Research Reserve.

Armal, S., Devineni, N., & Khanbilvardi, R. (2018). Trends in extreme rainfall frequency in the contiguous United States: Attribution to climate change and climate variability modes. *Journal of Climate, 31*(1), 369–385. https://doi.org/10.1175/JCLI-D-17-0106.1

Baranes, H., Dykstra, S. L., Jay, D. A., & Talke, S. A. (2023). Sea level rise and the drivers of daily water levels in the Sacramento-San Joaquin delta. *Scientific Reports*, *13*(1), 22454. https://doi.org/10.1038/s41598-023-49204-z

Beckley, B., Yang, X., Zelensky, N. P., Holmes, S. A., Lemoine, F. G., Ray, R. D., Mitchum, G. T., Desai, S., & Brown, S. T. (2024). Global Mean Sea Level Trend from Integrated Multi-Mission Ocean Altimeters TOPEX/Poseidon, Jason-1, OSTM/Jason-2, Jason-3, and Sentinel-6 Version 5.2. Ver. 5.2. PO. DAAC, CA, USA. https://doi.org/10.5067/GMSLM-TJ152. Accessed 03 Feb 2025.

Bevacqua, E., Maraun, D., Vousdoukas, M. I., Voukouvalas, E., Vrac, M., Mentaschi, L., & Widmann, M. (2019). Higher probability of compound flooding from precipitation and storm surge in Europe under anthropogenic climate change. *Science Advances*, *5*(9), 5531. https://doi.org/10.1126/sciadv.aaw5531

Blewitt, G., Hammond, W., & Kreemer, C. (2018). Harnessing the GPS data explosion for interdisciplinary science. *Eos*, *99*. https://doi.org/10.1073/pnas.2020943118

Codiga, D. L. (2011). Unified tidal analysis and prediction using the UTide matlab functions. https://doi.org/10.13140/RG.2.1.3761.2008

Dangendorf, S., Hendricks, N., Sun, Q., Klinck, J., Ezer, T., Frederikse, T., & Törnqvist, T. (2023). Acceleration of US Southeast and Gulf Coast sea-level rise amplified by internal climate variability. *Nature Communications*, *14*(1), 1–11. https://doi.org/10.1038/s41467-023-37649-9

De Leo, F., Talke, S. A., Orton, P. M., & Wahl, T. (2022). The effect of harbor developments on future high-tide flooding in Miami, Florida. *Journal of Geophysical Research: Oceans, 127*(7), e2022JC018496.

Dykstra, S. L., & Dzwonkowski, B. (2020). The propagation of fluvial flood waves through a backwater-estuarine environment. *Water Resources Research*, *56*(2). https://doi.org/10.1029/2019WR025743

Dykstra, S. L., & Dzwonkowski, B. (2021). The role of intensifying precipitation on coastal river flooding and compound river-storm surge events, Northeast Gulf of Mexico. *Water Resources Research*. https://doi.org/10.1029/2020wr029363

Dykstra, S. L., Dzwonkowski, B., & Torres, R. (2022). The role of river discharge and geometric structure on diurnal tidal dynamics, Alabama, USA. *Journal of Geophysical Research: Oceans*. https://doi.org/10.1029/2021jc018007

Dykstra, S. L., Ricche, G., Marmorino, G., & Yankovsky, A. E. (2024a). Forcing conditions of cross-shelf plumes on a wide continental shelf, Winyah Bay, South Atlantic bight. *Remote Sensing of Environment*, *311*, 114279. https://doi.org/10.1016/j.rse.2024.114279

Dykstra, S. L., Talke, S. A., Yankovsky, A. E., Torres, R., & Viparelli, E. (2024b). Reflection of storm surge and tides in convergent estuaries with Dams, the case of Charleston, USA. *Journal of Geophysical Research: Oceans*, *129*(9). https://doi.org/10.1029/2023jc020498

Elsinger, R. J., & Moore, W. S. (1984). ^{226}Ra and ^{228}Ra in the mixing zones of the Pee Dee River-Winyah Bay, Yangtze River and Delaware Bay estuaries. *Estuarine, Coastal and Shelf Science, 18*(6), 601–613.

Ensign, S. H., Hupp, C. R., Noe, G. B., Krauss, K. W., & Stagg, C. L. (2014). Sediment accretion in tidal freshwater forests and oligohaline marshes of the Waccamaw and Savannah Rivers, USA. *Estuaries and Coasts, 37*, 1107–1119.

Fant, C., Jacobs, J. M., Chinowsky, P., Sweet, W., Weiss, N., Sias, J. E., & Neumann, J. E. (2021). Mere nuisance or growing threat? The physical and economic impact of high tide flooding on US road networks. *Journal of Infrastructure Systems*, *27*(4), 04021044. https://doi.org/10.1061/(ASCE)IS.1943-555X.0000652

Feng, D., Tan, Z., Engwirda, D., Liao, C., Xu, D., Bisht, G., Zhou, Tian, Li, Hong-Yi., & Leung, L. R. (2022). Investigating coastal backwater effects and flooding in the coastal zone using a global river transport model on an unstructured mesh. *Hydrology and Earth System Sciences, 26*(21), 5473–5491. https://doi.org/10.5194/hess-26-5473-2022

Georgetown County (2024). Economic Development Element of the Comprehensive Plan. https://www.gtcounty.org/396/Comprehensive-Plan

Godin, G. (1999). The propagation of tides up rivers with special considerations on the upper Saint Lawrence River. *Estuarine, Coastal and Shelf Science, 48*(3), 307–324. https://doi.org/10.1006/ecss.1998.0422

Gori, A., Lin, N., & Smith, J. (2020). Assessing compound flooding from landfalling tropical cyclones on the North Carolina Coast. *Water Resources Research*, *56*(4). https://doi.org/10.1029/2019WR026788. e2019WR026788.

Griffin, M., Malsick, M., Mizzell, H., & Moore, L. (2019). Historic rainfall and record-breaking flooding from hurricane Florence in the Pee Dee watershed. *Journal of South Carolina Water Resources, 6*(1), 9. https://doi.org/10.34068/JSCWR.06.03

Guo, L., van der Wegen, M., Jay, D. A., Matte, P., Wang, Z. B., Roelvink, D., & He, Q. (2015). River-tide dynamics: Exploration of nonstationary and nonlinear tidal behavior in the Yangtze River estuary. *Journal of Geophysical Research. Oceans, 120*(5), 3499–3521. https://doi.org/10.1002/2014jc010491

Hague, B. S., McGregor, S., Jones, D. A., Reef, R., Jakob, D., & Murphy, B. F. (2023). The global drivers of chronic coastal flood hazards under sea-level rise. *Earth's Future*, *11*(8). https://doi.org/10.1029/2023EF003784. e2023EF003784.

Hague, B. S., & Talke, S. A. (2024). The influence of future changes in tidal range, storm surge, and mean sea level on the emergence of chronic flooding. *Earth's Future*, *12*(2), e2023EF003993. https://doi.org/10.1029/2023EF003993

Hamlington, B. D., Bellas-Manley, A., Willis, J. K., & Kopp, R. (2024). The rate of global sea level rise doubled during the past three decades. *Commun Earth Environ*, *5*, 601. https://doi.org/10.1038/s43247-024-01761-5

Hamlington, B. D., Chambers, D. P., Frederikse, T., Dangendorf, S., Fournier, S., Buzzanga, B., & Nerem, R. S. (2022). Observation-based trajectory of future sea level for the coastal United States tracks near high-end model projections. *Communications Earth & Environment, 3*(1), 230.

Helaire, L. T., Talke, S. A., Jay, D. A., & Chang, H. (2020). Present and future flood hazard in the lower Columbia River Estuary: Changing flood hazards in the Portland-Vancouver Metropolitan area. J*ournal of Geophysical Research: Oceans, 125*(7), e2019JC015928.

Helaire, L. T., Talke, S. A., Jay, D. A., & Mahedy, D. (2019). Historical changes in Lower Columbia River and estuary floods: A numerical study. *Journal of Geophysical Research. Oceans, 124*(11), 7926–7946.

Hino, M., Belanger, S. T., Field, C. B., Davies, A. R., & Mach, K. J. (2019). High-tide flooding disrupts local economic activity. *Science Advances*, *5*(2), eaau2736. https://doi.org/10.1126/sciadv.aau2736

Jafarzadegan, K., Moradkhani, H., Pappenberger, F., Moftakhari, H., Bates, P., Abbaszadeh, P., & Duan, Q. (2023). Recent advances and new frontiers in riverine and coastal flood modeling. *Reviews of Geophysics*, *61*(2), e2022RG000788. https://doi.org/10.1029/2022RG000788.

Jay, D. A., Borde, A. B., & Diefenderfer, H. L. (2016). Tidal-fluvial and estuarine processes in the Lower Columbia River: II. Water level models, floodplain wetland inundation, and system zones. *Estuaries and Coasts, 39*, 1299–1324. https://doi.org/10.1007/s12237-016-0082-4

Jay, D. A., & Flinchem, E. P. (1997). Interaction of fluctuating river flow with a barotropic tide: A demonstration of wavelet tidal analysis methods. *Journal of Geophysical Research. Oceans, 102*(C3), 5705–5720.

Jay, D. A., Leffler, K., & Degens, S. (2011). Long-term evolution of Columbia River tides. *Journal of Waterway, Port, Coastal, and Ocean Engineering, 137*(4), 182–191. https://doi.org/10.1061/(ASCE)WW.1943-5460.0000082

Karegar, M. A., Dixon, T. H., & Engelhart, S. E. (2016). Subsidence along the Atlantic Coast of North America: Insights from GPS and late Holocene relative sea level data. *Geophysical Research Letters, 43*(7), 3126–3133. https://doi.org/10.1002/2016GL068015

Kim, Y. H., & Voulgaris, G. (2005). Effect of channel bifurcation on residual estuarine circulation: Winyah Bay, South Carolina. *Estuarine, Coastal and Shelf Science, 65*(4), 671–686. https://doi.org/10.1016/j.ecss.2005.07.004

Kukulka, T., & Jay, D. A. (2003). Impacts of Columbia river discharge on salmonid habitat: 1. A nonstationary fluvial tide model. *Journal of Geophysical Research: Oceans*, *108*(C9). https://doi.org/10.1029/2002JC001382

Kumbier, K., Carvalho, R. C., & Woodroffe, C. D. (2018). Modelling hydrodynamic impacts of Sea-Level rise on Wave-Dominated Australian estuaries with differing geomorphology. *Journal of Marine Science and Engineering*, *6*(2), 66. https://doi.org/10.3390/jmse6020066

Leijnse, T., van Ormondt, M., Nederhoff, K., & Van Dongeren, A. (2021). Modeling compound flooding in coastal systems using a computationally efficient reduced-physics solver: Including fluvial, pluvial, tidal, wind-and wave-driven processes. *Coastal Engineering*, *163*, 103796. https://doi.org/10.1016/j.coastaleng.2020.103796

Li, S., Wahl, T., Barroso, A., Coats, S., Dangendorf, S., Piecuch, C., & Liu, L. (2022). Contributions of different sea-level processes to high-tide flooding along the US coastline. *Journal of Geophysical Research: Oceans*, *127*(7). https://doi.org/10.1029/2021JC018276. e2021JC018276.

Li, S., Wahl, T., Talke, S. A., Jay, D. A., Orton, P. M., Liang, X., & Liu, L. (2021). Evolving tides aggravate nuisance flooding along the US coastline. *Science Advances*, *7*(10), eabe2412. https://doi.org/10.1126/sciadv.abe2412

Matte, P., Jay, D. A., & Zaron, E. D. (2013). Adaptation of classical tidal harmonic analysis to nonstationary tides, with application to river tides. *Journal of Atmospheric and Oceanic Technology*, *30*(3), 569–589. https://doi.org/10.1175/JTECH-D-12-00016.1

McKeon, K., & Piecuch, C. G. (2025). Compound minor floods and the role of discharge in the Delaware river estuary. *Journal of Geophysical Research: Oceans*. https://doi.org/10.1029/2024JC021716., 130, e2024JC021716.

Moftakhari, H., Muñoz, D. F., Asanjan, A. A., AghaKouchak, A., Moradkhani, H., & Jay, D. A. (2024). Nonlinear interactions of Sea-Level rise and storm tide alter extreme coastal water levels: How and why? *AGU Advances*, *5*(2). https://doi.org/10.1029/2023av000996

Moftakhari, H. R., AghaKouchak, A., Sanders, B. F., Feldman, D. L., Sweet, W., Matthew, R. A., & Luke, A. (2015). Increased nuisance flooding along the coasts of the United States due to sea level rise: Past and future. *Geophysical Research Letters, 42*(22), 9846–9852. https://doi.org/10.1002/2015GL066072

Moftakhari, H. R., AghaKouchak, A., Sanders, B. F., & Matthew, R. A. (2017). Cumulative hazard: The case of nuisance flooding. *Earth's Future, 5*(2), 214–223.

Moftakhari, H., Schubert, J. E., AghaKouchak, A., Matthew, R. A., & Sanders, B. F. (2019). Linking statistical and hydrodynamic modeling for compound flood hazard assessment in tidal channels and estuaries. *Advances in Water Resources*, *128*, 28–38. https://doi.org/10.1016/j.advwatres.2019.04.009

Moore, F. C., & Obradovich, N. (2020). Using remarkability to define coastal flooding thresholds. *Nature Communications*, *11*, 530. https://doi.org/10.1038/s41467-019-13935-3

Morris, J., & Renken, K. (2020). Past, present, and future nuisance flooding on the Charleston Peninsula. *Plos One*, *15*(9), e0238770. https://doi.org/10.1371/journal.pone.0238770

Nederhoff, K., Saleh, R., Tehranirad, B., Herdman, L., Erikson, L., Barnard, P. L., & Van der Wegen, M. (2021). Drivers of extreme water levels in a large, urban, high-energy coastal estuary – A case study of the San Francisco Bay. *Coastal Engineering*, *170*, 103984. https://doi.org/10.1016/j.coastaleng.2021.103984

Nerem, R. S., Beckley, B. D., Fasullo, J. T., Hamlington, B. D., Masters, D., & Mitchum, G. T. (2018). Climate-change–driven accelerated sea-level rise detected in the altimeter era. *Proceedings of the National Academy of Sciences of the United States of America, 115*(9), 2022–2025. https://doi.org/10.1073/pnas.1717312115

Noble, M. A., & Gelfenbaum, G. R. (1992). Seasonal fluctuations in sea level on the South Carolina Shelf and their relationship to the Gulf Stream. *Journal of Geophysical Research, 97*(C6), 9521–9529.

Oelsmann, J., Marcos, M., Passaro, M., Sanchez, L., Dettmering, D., Dangendorf, S., & Seitz, F. (2024). Regional variations in relative sea-level changes influenced by nonlinear vertical land motion. *Nature Geoscience*, *17*(2), 137–144. https://doi.org/10.1038/s41561-023-01357-2

Ohenhen, L. O., Shirzaei, M., & Barnard, P. L. (2024). Slowly but surely: Exposure of communities and infrastructure to subsidence on the US East Coast. *PNAS Nexus*, *3*(1), pgad426. https://doi.org/10.1093/pnasnexus/pgad426

Orton, P. M., Conticello, F. R., & Cioffi, F. (2020). Flood hazard assessment from storm tides, rain and sea level rise for a tidal river estuary. *Natural Hazards, 102*, 729–757.

Pareja-Roman, L. F., Orton, P. M., & Talke, S. A. (2023). Effect of estuary urbanization on tidal dynamics and high tide flooding in a coastal lagoon. *Journal of Geophysical Research: Oceans, 128*(1), e2022JC018777.

Parker, B. B. (2007). Tidal analysis and prediction. *NOAA special publication NOS CO-OPS 3* (p. 378). National Oceanic and Atmospheric Administration.

Patchineelam, S. M., Kjerfve, B., & Gardner, L. R. (1999). A preliminary sediment budget for the Winyah Bay estuary, South Carolina, USA. *Marine Geology, 162*(1), 133–144. https://doi.org/10.1016/S0025-3227(99)00059-6

Piecuch, C. G., Bittermann, K., Kemp, A. C., Ponte, R. M., Little, C. M., Engelhart, S. E., & Lentz, S. J. (2018). River-discharge effects on United States Atlantic and Gulf coast sea-level changes. *Proceedings of the National Academy of Sciences, 115*(30), 7729–7734. https://doi.org/10.1073/pnas.1805428115

Piecuch, C. G., Das, S. B., Gorrell, L., Dangendorf, S., Hamlington, B. D., Thompson, P. R., & Wahl, T. (2025). Impact-based thresholds for investigation of high-tide flooding in the united States. *Earth's Future*, *13*(4). https://doi.org/10.1029/2024EF005850. e2024EF005850.

Pietrafesa, L. J., Zhang, H., Bao, S., Gayes, P. T., & Hallstrom, J. O. (2019). Coastal flooding and inundation and inland flooding due to downstream blocking. *Journal of Marine Science and Engineering*, *7*(10), 336. https://doi.org/10.3390/jmse7100336

Rahimi, R., Tavakol-Davani, H., Graves, C., Gomez, A., & Fazel Valipour, M. (2020). Compound inundation impacts of coastal climate change: Sea-level rise, groundwater rise, and coastal precipitation. *Water*, *12*(10), 2776. https://doi.org/10.3390/w12102776

Ralston, D. K., Talke, S., Geyer, W. R., Al-Zubaidi, H. A., & Sommerfield, C. K. (2019). Bigger tides, less flooding: Effects of dredging on barotropic dynamics in a highly modified estuary. *Journal of Geophysical Research. Oceans, 124*(1), 196–211.

Ruhl, C. A., & Simpson, M. R. (2005). *Computation of discharge using the index-velocity method in tidally affected areas* (Vol. 2005). US Department of the Interior, US Geological Survey.

Serafin, K. A., Ruggiero, P., Parker, K., & Hill, D. F. (2019). What's streamflow got to do with it? A probabilistic simulation of the competing oceanographic and fluvial processes driving extreme along-river water levels. *Natural Hazards and Earth System Sciences, 19*(7), 1415–1431.

Suttles, K. M., Singh, N. K., Vose, J. M., Martin, K. L., Emanuel, R. E., Coulston, J. W., Saia, S. M., & Crump, M. T. (2018). Assessment of hydrologic vulnerability to urbanization and climate change in a rapidly changing watershed in the Southeast US. *Science of the Total Environment, 645*, 806–816. https://doi.org/10.1016/j.scitotenv.2018.06.287

Sweet, W., Dusek, G., Obeysekera, J., & Marra, J. (2018). Patterns and projections of high tide flooding along the US coastline using a common impact threshold. NOAA Technical Report NOS CO-OPS 086.

Sweet, W., & Park, J. (2014). From the extreme to the mean: Acceleration and tipping points of coastal inundation from sea level rise. *Earth's Future, 2*(12), 579–600. https://doi.org/10.1002/2014ef000272

Sweet, W., Simon, S., Dusek, G., Marcy, D., & Marra, J. (2021). 2021 State of High Tide Flooding and Annual Outlook. https://doi.org/10.25923/mx62-rx21

Talke, S. A. (2025). How tidal properties influence the future duration of coastal flooding. *npj Natural Hazards, 2*(1), Article 36. https://doi.org/10.1038/s44304-025-00086-3

Talke, S. A., Familkhalili, R., & Jay, D. A. (2021). The influence of channel deepening on tides, river discharge effects, and storm surge. *Journal of Geophysical Research: Oceans*, *126*(5), e2020JC016328. https://doi.org/10.1029/2020JC016328

Tedesco, M., McAlpine, S., & Porter, J. R. (2020). Exposure of real estate properties to the 2018 hurricane Florence flooding. *Natural Hazards and Earth System Sciences, 20*, 907–920. https://doi.org/10.5194/nhess-20-907-2020

Tehranirad, B., Herdman, L., Nederhoff, K., Erikson, L., Cifelli, R., Pratt, G., & Barnard, P. (2020). Effect of fluvial discharges and remote non-tidal residuals on compound flood forecasting in San Francisco Bay. *Water*, *12*(9), 2481. https://doi.org/10.3390/w12092481

Templeton, W. J., Jay, D. A., Diefenderfer, H. L., & Talke, S. A. (2024). Shallow-water habitat in the lower Columbia River estuary: A highly altered system. *Estuaries and Coasts, 47*(1), 91–116. https://doi.org/10.1007/s12237-023-01229-3

Thompson, P. R., Widlansky, M. J., Hamlington, B. D., Merrifield, M. A., Marra, J. J., Mitchum, G. T., & Sweet, W. (2021). Rapid increases and extreme months in projections of United States high-tide flooding. *Nature Climate Change, 11*(7), 584–590. https://doi.org/10.1038/s41558-021-01077-8

Thompson, P. R., Widlansky, M. J., Merrifield, M. A., Becker, J. M., & Marra, J. J. (2019). A statistical model for frequency of coastal flooding in Honolulu, Hawaii, during the 21st century. *Journal of Geophysical Research. Oceans, 124*(4), 2787–2802. https://doi.org/10.1029/2018jc014741

Van De Plassche, O., Wright, A. J., Horton, B. P., Engelhart, S. E., Kemp, A. C., Mallinson, D., & Kopp, R. E. (2014). Estimating tectonic uplift of the Cape Fear Arch (south-eastern United States) using reconstructions of Holocene relative sea level. *Journal of Quaternary Science, 29*(8), 749–759. https://doi.org/10.1002/jqs.2746

Visit Myrtle Beach (2022). https://www.visitmyrtlebeach.com/media/media-resources/fact-sheet#:~:text=Home%20to%20world%2Dclass%20golf,over%2017%20million%20visitors%20annually.

Wahl, T., Jain, S., Bender, J., Meyers, S. D., & Luther, M. E. (2015). Increasing risk of compound flooding from storm surge and rainfall for major US cities. *Nature Climate Change*, *5*(12), 1093–1097. https://doi.org/10.1038/nclimate2736

Xiao, Z., Yang, Z., Wang, T., Sun, N., Wigmosta, M., & Judi, D. (2021). Characterizing the Non-Linear interactions between Tide, storm Surge, and river flow in the Delaware Bay Estuary, united States. *Frontiers in Marine Science*, *8*, 715557. https://doi.org/10.3389/fmars.2021.715557

Yin, J. (2023). Rapid decadal acceleration of sea level rise along the US East and Gulf Coasts during 2010–22 and its impact on hurricane-induced storm surge. *Journal of Climate*, *36*(13), 4511–4529. https://doi.org/10.1175/JCLI-D-22-0670.1